

---

# Surprises in adversarially-trained linear regression

---

Antônio H. Ribeiro\*, Dave Zachariah, Thomas B. Schön  
Department of Information Technology  
Uppsala University

## Abstract

State-of-the-art machine learning models can be vulnerable to very small input perturbations that are adversarially constructed. Adversarial training is one of the most effective approaches to defend against such examples. We show that for linear regression problems, adversarial training can be formulated as a convex problem. This fact is then used to show that  $\ell_\infty$ -adversarial training produces sparse solutions and has many similarities to the lasso method. Similarly,  $\ell_2$ -adversarial training has similarities with ridge regression. We use a robust regression framework to analyze and understand these similarities and also point to some differences. Finally, we show how adversarial training behaves differently from other regularization methods when estimating overparameterized models (i.e., models with more parameters than datapoints). It minimizes a sum of three terms which regularizes the solution, but unlike lasso and ridge regression, it can sharply transition into an interpolation mode. We show that for sufficiently many features or sufficiently small regularization parameters, the learned model perfectly interpolates the training data while still exhibiting good out-of-sample performance.

## 1 Introduction

Robustness is a fundamental goal in machine learning that often surpasses that of achieving high performance in a controlled scenario. Indeed, the brittleness of modern machine learning models presents a challenge to their deployment in critical situations. The framework of adversarial attacks has generated striking examples of their vulnerability, where very small input perturbations can cause a substantial performance drop in otherwise state-of-the-art models, see for instance [1]–[6]. It considers inputs contaminated with disturbances deliberately chosen to maximize the model error when compared to the initial and correct prediction. The study of adversarial attacks pre-dates the widespread use of deep neural networks [7], [8]. Nonetheless, the susceptibility of state-of-the-art deep learning models to very small input modifications gave the framework higher visibility.

Adversarial training [9] is one of the most effective approaches for deep learning models to defend against adversarial attacks. The topic was extensively studied by the research community, see [9]–[11]. The idea is straightforward: It considers the situation where the training samples have been modified by an adversary. Since training samples are adversarially perturbed it is expected that the model will be more robust when faced with new adversarially perturbed samples. Mathematically, adversarial training is formulated as a min-max problem, searching for the best solution to the worst-case attacks.

To a large extent, deep learning models have been a central focus in the study of adversarial training. In this paper, we take one step back and study the properties of adversarial training in linear regression. There is a strong reason for this focus, for regression and linear models adversarial training can be formulated in a convex and quadratic form [12]. We show that this simplification opens up for a deeper study of adversarial attacks and it also reveals interesting behavior that can pass unnoticed

---

\*E-mail: antonio.horta.ribeiro@it.uu.se

when considering a more general nonlinear min-max problem, for which it is hard to obtain global optima and provide thorough analysis.

Equipped with this perspective, this paper makes the following contributions:

1. We observe that  $\ell_\infty$ -adversarial training produces sparse solutions and can behave similar to lasso when there are not too many parameters. Similarly,  $\ell_2$ -adversarial training has many similarities to ridge regression.
2. We show that adversarial training is an instance of robust regression and show how to use this insight to compare adversarial training with lasso.
3. We study the behavior of adversarial training in overparameterized models, where there are more parameters than data. We observe that adversarial training exhibits an interesting behavior of both regularizing the solution while *also interpolating the training data* in certain regimes.

## 2 Related work

**Adversarial training in linear models.** While most papers appear to be interested in adversarial training for neural networks, there are still several papers studying different properties of adversarial training in linear models. Taheri *et al.* [13] derived asymptotics for adversarial training in binary classification. Javanmard *et al.* [14] provide asymptotics for adversarial training in linear regression, Javanmard *et al.* [15] study it in classification settings and Hassani *et al.* [16] for random feature regressions. Min *et al.* [17] study how the dataset size affects adversarial performance. Yin *et al.* [18] provides an analysis of  $\ell_\infty$ -attack on linear classifiers based on the Rademacher complexity.

While there was initial speculation that the highly nonlinear nature of deep neural networks was the cause of its vulnerabilities to attacks [1] the idea was later dismissed. Indeed, Goodfellow *et al.* [2] shows that the existence of vulnerabilities to adversarial attacks can be explained and observed in a purely linear setting and the high dimensionality is pointed out as a main cause of the problem.

**Adversarial training and sparsity.** There are studies highlighting that sparse models can be more robust to adversarial attacks [19], [20]. Xing *et al.* [21] propose to add an  $\ell_1$ -penalty to the adversarial loss to improve generalization. We could not find a clear reference for the fact  $\ell_\infty$ -adversarial attacks yield sparse solutions in linear regression, although several researchers in correspondence seem to intuitively expect it. Related facts have since long been established for robust regression [22] and in Section 5 we show how adversarial training differs. Framing adversarial training as a robust optimization problem is also commonplace [9], [23].

**Overparameterization.** The seminal work by Belkin *et al.* [24] has shown an interesting line of reasoning that help explain how very rich models such as neural networks that are trained to exactly fit the data can still generalize well into new datapoints. Indeed, increasing the model size has been a standard strategy in obtaining better models of this type and it remains one of the big puzzles surrounding them [25]. The study of the so-called *double-descent* phenomenon [24] and benign overfitting [26] has produced intense research about the properties of overparameterized models [27]. A natural next step is to ask whether overparameterized models can be robust and indeed the relation between high dimensionality and adversarial attacks and possible conflicts between robustness and performance is further explored by [5], [12], [18], [28]. Javanmard *et al.* [15] studies how overparameterization affects robustness to perturbations. Min *et al.* [17] studies how the size of the dataset affects adversarial performance.

## 3 Background and problem formulation

### 3.1 Setup

Consider a training dataset  $\{(x_i, y_i)\}_{i=1}^n$  consisting of  $n$  i.i.d. datapoints of dimension  $\mathbb{R}^m \times \mathbb{R}$ , sampled from the distribution  $(x_i, y_i) \sim P_{x,y}$ . To this data, we fit a *linear model* from the function class  $\{\beta^\top x \mid \beta \in \mathbb{R}^m\}$ . Let  $(x_0, y_0) \sim P_{x,y}$  be an independently drawn test point. We will use subscripts to denote the source of randomness considered in the conditional expectation. For instance, let  $x, y, z, w$  be random variables, we use  $\mathbb{E}_{x,y}[f(x, y, z, w)]$  to denote the expectation with respect

to  $x, y$  and conditioned on the variables that are not explicitly mentioned in the subscript, here  $z$  and  $w$ . Using this notation, we denote the out-of-sample *prediction risk* by

$$R(\beta) = \mathbb{E}_{x_0, y_0} [(y_0 - x_0^\top \beta)^2]. \quad (1)$$

The  $\ell_p$  *adversarial risk* is defined as

$$R_p^{\text{adv}}(\beta) = \mathbb{E}_{x_0, y_0} \left[ \max_{\|\Delta x_0\|_p \leq \delta} (y_0 - (x_0 + \Delta x_0)^\top \beta)^2 \right], \quad (2)$$

which is the risk when the model is subject to an adversarial disturbance  $\Delta x_0$  that results in the worst possible performance for any given  $\beta$ . The disturbance is bounded in a region  $\|\Delta x_0\|_p \leq \delta$ , where  $\|\cdot\|_p$  denotes the  $\ell_p$  norm of a vector.

**Definition 1** (Vector  $p$ -norms). *Let  $a \in \mathbb{R}^n$  and  $p \in \mathbb{R}, p \geq 1$ , the  $p$ -norm of this vector is defined as:*

$$\|a\|_p = \left( \sum_{i=1}^n |a_i|^p \right)^{\frac{1}{p}}, \quad (3)$$

and  $\|a\|_\infty = \max_{1 \leq i \leq n} |a_i|$ .

### 3.2 Adversarial training

Empirical risk minimization (ERM) has been tremendously successful as a recipe for finding predictors with good performance. Here we denote the *empirical risk* by

$$\widehat{R}(\beta) = \frac{1}{n} \sum_{i=1}^n (y_i - x_i^\top \beta)^2, \quad (4)$$

where the expectation w.r.t. the true distribution has been replaced by the average over the observed training samples. Adversarial training relies on the natural idea of trying to obtain models that are more robust to adversarial attacks by minimizing the *empirical adversarial risk*,

$$\widehat{R}_p^{\text{adv}}(\beta) = \frac{1}{n} \sum_{i=1}^n \max_{\|\Delta x_i\|_p \leq \delta} (y_i - (x_i + \Delta x_i)^\top \beta)^2 \quad (5)$$

rather than the traditional risk.

### 3.3 Properties of the adversarial risk in linear regression

We will rely on the result—derived by Ribeiro *et al.* [12]—that the adversarial risk for linear regression can be simplified to a quadratic form. The result is stated in the next lemma. The proof is based on Hölder’s inequality  $|\beta^\top \Delta x| \leq \|\beta\|_p \|\Delta x\|_q$  and on the fact that we can, given  $\beta$ , construct  $\Delta x$  such that the equality holds (see the Supplementary Material for more details).

**Lemma 2** (Ribeiro *et al.* [12]). *Let  $q \geq 1$  for which  $\frac{1}{p} + \frac{1}{q} = 1$ ,<sup>2</sup> then*

$$R_p^{\text{adv}}(\beta) = \mathbb{E}_{x_0, y_0} \left[ (|y_0 - x_0^\top \beta| + \delta \|\beta\|_q)^2 \right]. \quad (6)$$

This lemma can be used to show the convexity of the adversarial risk.

**Proposition 3** (Ribeiro *et al.* [12]). *For  $p \in [1, \infty]$ ,  $R_p^{\text{adv}}(\beta)$  is convex in  $\beta$ .*

We note that all the results obtained for the adversarial risk are also valid for the empirical adversarial risk. So it follows from Lemma 2 that:

$$\widehat{R}_p^{\text{adv}}(\beta) = \frac{1}{n} \sum_{i=1}^n (|y_i - x_i^\top \beta| + \delta \|\beta\|_q)^2 \quad (7)$$

and minimizing the risk is a *convex problem*.

<sup>2</sup>The result still holds for the pair of values  $(p = 1, q = \infty)$  and  $(p = \infty, q = 1)$ .

## 4 Adversarial training and regularization

Lemma 2 provides an easy-to-analyse formula for the adversarial risk. By expanding and using the linearity of the expectation we obtain:

$$R_p^{\text{adv}}(\beta) = R(\beta) + 2\delta\|\beta\|_q \mathbb{E}_{x_0, y_0} [|y_0 - x_0^\top \beta|] + \delta^2\|\beta\|_q^2. \quad (8)$$

When the middle term in Eq. (8) is small, the above expression implies that  $R_p^{\text{adv}}(\beta) \approx R(\beta) + \delta^2\|\beta\|_q^2$ . The notion will be formalized in a moment. For now, we just notice that the right-hand side of the approximation  $R_2^{\text{adv}}(\beta) \approx R(\beta) + \delta^2\|\beta\|_2^2$  is the cost function in ridge regression, and  $R_\infty^{\text{adv}}(\beta) \approx R(\beta) + \delta^2\|\beta\|_1^2$  is equivalent to that in lasso (i.e., it is an alternative Lagrangian formulation of the constrained lasso). It is natural to wonder about the similarities and differences between the estimators obtained in each case. The next example illustrates a case where they are indeed very similar.

### Example: diabetes progression

Here we will study the solutions of adversarial training in the Diabetes dataset [29], which was used to study lasso. Here, we use it to show similarities between adversarial training and other methods. We will focus our experiments on adversarial attacks for  $p = 2$  and  $p = \infty$ . The dataset has  $m = 10$  baseline variables (age, sex, body mass index, average blood pressure, and six blood serum measurements), which were obtained for  $n = 442$  diabetes patients. The model output is a quantitative measure of the disease progression one year after the baseline variables were measured.

We compare adversarial training to

ridge regression and lasso regression [30]. Ridge regression minimizes  $(\hat{R}(\beta) + \delta\|\beta\|_2^2)$  and lasso minimizes  $(\hat{R}(\beta) + \delta\|\beta\|_1)$ . The empirical adversarial risk (7) is convex in  $\beta$  and readily minimized to obtain the adversarial training solution. All our numerical examples in this paper are implemented using CVXPY [31]. In Fig. 1 we show the so-called regularization paths for the different methods. The plot shows the value of the coefficient estimates as we vary the regularization parameter  $\delta$ . We compute the regularization path of ridge regression and adversarial training by solving the optimization problem for a grid of 200 values of  $\delta$  equally spaced in the logarithmic space. For lasso, we use the coordinate descent algorithm proposed by [32]. The result is displayed for the different methods and, as  $\delta \rightarrow \infty$ , the coefficients should approach zero for all methods. On the other hand, as  $\delta \rightarrow 0$ , the coefficients should approach the least-squares solution.

A visual inspection of the regularization paths for ridge regression, in panel (a), and  $\ell_2$ -adversarial training, in panel (b), shows the similarities between the results obtained from the two methods. One interesting difference is that while ridge regression coefficients slowly decay to zero as the amount of regularization is increased, the transition is more abrupt in the case of  $\ell_2$ -adversarial training. At  $\delta \approx 10^{-0.5}$ , we see all coefficients collapsing to zero. Comparing panel (c) and (d), similarities between lasso and  $\ell_\infty$ -adversarial training also becomes evident. The fact that  $\ell_\infty$ -adversarial training yield sparse solution is shown in Fig. 1(d). Moreover, the regularization path for  $\ell_\infty$ -adversarial training is remarkably similar to the one obtained using lasso.

**Adversarial risk envelope** Here we formalize the approximation mentioned at the beginning of this section. Specifically, the adversarial risk is bounded as follows:

$$R(\beta) + \delta^2\|\beta\|_q^2 \leq R_p^{\text{adv}}(\beta) \leq \left(\sqrt{R(\beta)} + \delta\|\beta\|_q\right)^2. \quad (9)$$

The lower bound follows from the fact that the middle term in (8) is non-negative and the upper bound follows from Jensen’s inequality. The optimization problem we would have by trying to

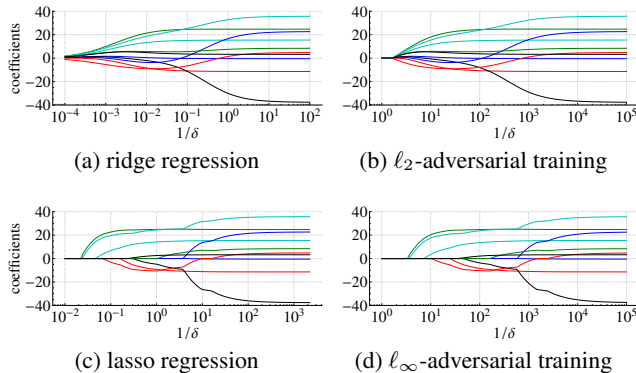


Figure 1: **Regularization paths.** On the horizontal axis we give the inverse of the regularization parameter (in log scale). On the vertical axis we show the coefficients of the learned linear model.

minimize either the upper or lower envelope are equivalent in the following sense: they are both Lagrangian formulations of the same constrained problem:  $\min R(\beta)$  subject to  $\|\beta\|_q \leq \lambda$  given an appropriate choice of  $\lambda$ .

It is natural to wonder, when analysing the minimizer of the envelopes actually provide insight into the minimizer of the adversarial risk. One example where the function is uniquely determined by the envelopes is when  $(x_0, y_0)$  are jointly zero-mean Gaussian. In this case,  $y_0 - x_0^\top \beta$  is also Gaussian, which has a known mean absolute deviation:  $\mathbb{E}_{x_0, y_0} [|y_0 - x_0^\top \beta|] = \sqrt{\frac{2}{\pi}} R(\beta)$ . Hence, if we denote the upper envelope by  $G(\beta)$  and the lower envelope by  $g(\beta)$ , the adversarial risk is in this case a weighted average of the two envelopes  $R_p^{\text{adv}}(\beta) = \left(1 - \sqrt{\frac{2}{\pi}}\right) g(\beta) + \sqrt{\frac{2}{\pi}} G(\beta)$ . The diabetes example above also gives an example where the minimizers of the empirical adversarial risk is similar to that of lasso and ridge regression, which in turn are related to the envelope solutions.

## 5 Robust regression

To get a better understanding of the similarities and differences with lasso, we investigate adversarial training through the lens of robust regression. Let  $X \in \mathbb{R}^{n \times m}$  denote the matrix consisting of stacked training inputs  $x_i^\top$  and similarly we let  $y \in \mathbb{R}^n$  denote the vector of outputs. In robust linear regression, the cost function being minimized during training is

$$\widehat{R}_{\mathcal{S}}^{\text{robust}}(\beta) = \max_{\Delta \in \mathcal{S}} \|y - (X + \Delta)^\top \beta\|_2, \quad (10)$$

where  $\mathcal{S}$  denotes the ‘uncertainty set’ and the disturbance matrix  $\Delta$  is constrained to belong to this set.

A well-known fact is that robust regression can be equivalent to lasso. Following Xu *et al.* [22], we consider the following uncertainty set:

$$\mathcal{C}_2 = \left\{ \begin{bmatrix} \left| \right| & & \left| \right| \\ \zeta_1 & \cdots & \zeta_m \\ \left| \right| & & \left| \right| \end{bmatrix} : \|\zeta_i\|_2 \leq \delta \text{ for } i = 1, \dots, m \right\} \quad (11)$$

where we use  $\mathcal{C}_2$  to highlight that the columns of the disturbance matrix have their  $\ell_2$ -norm bounded. The next proposition establishes how for this set robust optimization is equivalent to lasso.

**Proposition 4** (Xu *et al.* [22]). *Let the uncertainty set be defined as in Eq. (11) i.e.,  $\mathcal{S} = \mathcal{C}_2$  then the robust optimization cost reduces to:*

$$\widehat{R}_{\mathcal{C}_2}^{\text{robust}}(\beta) = \|y - X\beta\|_2 + \delta \|\beta\|_1. \quad (12)$$

The equivalence of the solution to the above problem and lasso follows from the fact that they are both Lagrangian formulations of equivalently constrained optimization problems. The proof of the proposition follow from Xu *et al.* [22, Theorem 1].

Now, let us instead consider the following alternative uncertainty set

$$\mathcal{R}_p = \left\{ \begin{bmatrix} \text{---} & \Delta x_1 & \text{---} \\ & \vdots & \\ \text{---} & \Delta x_m & \text{---} \end{bmatrix} : \|\Delta x_i\|_p \leq \delta \text{ for } i = 1, \dots, m \right\}. \quad (13)$$

For this uncertainty set, the next proposition provides the equivalence of robust regression and our definition of adversarial training.

**Proposition 5.** *A vector  $\beta$  minimizes the robust regression cost for the uncertainty set defined in (13)  $\mathcal{S} = \mathcal{R}_p$  if and only if it is minimizer of the empirical adversarial risk  $\widehat{R}_p^{\text{adv}}(\beta)$  defined in (5). That is,*

$$\arg \min_{\beta} \widehat{R}_p^{\text{adv}}(\beta) = \arg \min_{\beta} \widehat{R}_{\mathcal{R}_p}^{\text{robust}}(\beta). \quad (14)$$

*Proof.* From Eq. (5) it follows that:

$$\widehat{R}_p^{\text{adv}}(\beta) = \frac{1}{n} \max_{\Delta \in \mathcal{R}_p} \|y - (X + \Delta)\beta\|_2^2 = \frac{1}{n} \left( \max_{\Delta \in \mathcal{R}_p} \|y - (X + \Delta)\beta\|_2 \right)^2$$

Where we used in the last equality that the function  $h(z) = \frac{1}{n}z^2$  is monotonically increasing for  $z \geq 0$ . Repeating the same argument, but now for the minimization, yields that  $\widehat{R}_p^{\text{adv}}(\beta)$  has the same minimizer as  $\max_{\Delta \in \mathcal{R}_p} \|y - (X + \Delta)\beta\|_2$ .  $\square$

In summary, robust regression is equivalent to lasso for so called ‘feature-wise uncoupled’ uncertainty sets  $\mathcal{C}_2$ , where the norm of the perturbation *for each feature* is (independently) constrained. Adversarial training, on the other hand, considers ‘sample-wise uncoupled’ uncertainty sets  $\mathcal{R}_p$ , where the norm of the perturbation *for each sample* is (independently) constrained.

## 6 Overparameterized models

Fig. 1 illustrates a scenario where the distinction between adversarial training and other regularization methods is minimal. There, lasso and the  $\ell_\infty$  adversarial training yielding quite similar regularization paths. Similarly, ridge and  $\ell_2$  adversarial training also behave almost the same. In this section, we show this is not always the case and that the two formulations can behave qualitatively differently. We will focus on the behavior of the method in the overparameterized region.

### 6.1 Can interpolation and regularization coexist?

To study the behavior of adversarial training in the overparameterized region, we will consider artificially generated data. We consider the features are generated from a given distribution and the output is computed as a linear combination of these features plus some additive noise:

$$y_i = x_i^\top \beta + \epsilon_i. \quad (15)$$

Here, we consider independent Gaussian noise and covariates:  $\epsilon_i \sim \mathcal{N}(0, \sigma^2)$  and  $x_i \sim \mathcal{N}(0, r^2 I_m)$ . We keep the signal-to-noise ratio constant with  $m$  by scaling the parameter  $\beta$  by  $1/\sqrt{m}$  so that  $\mathbb{E}[x_i^\top \beta]$  is constant. In Supplementary Material Section C we consider a different data model that uses features that are noisy observations of a lower-dimensional subspace, similar to [33, Section 5.4].

Fig. 2 shows the training mean square error (MSE) of the learned predictors. We keep the number of training datapoints constant and vary the number of features  $m$ . The behavior of adversarial training is significantly different from ridge regression and lasso. For instance, in Fig. 2(b) we see that for  $\ell_2$ -adversarial training there is an abrupt transition from a small training error to virtually zero training error (up to numerical precision of  $10^{-20}$ ).

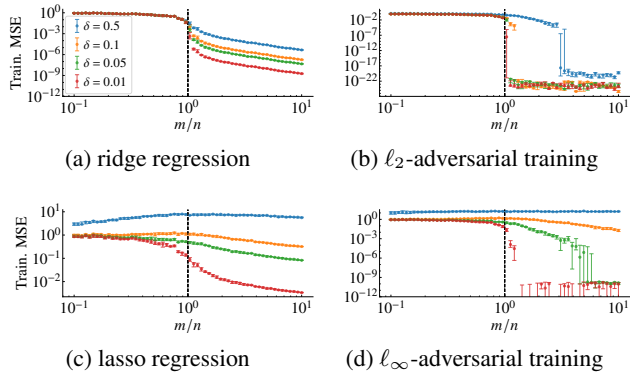


Figure 2: **Mean square error in training data.** The error bars give the median and the 0.25 and 0.75 quantiles obtained from numerical experiment (10 realizations) and for regularization parameter  $\delta = \{0.5, 0.1, 0.05, 0.01\}$  with the colors corresponding to each case indicated in the legend. We use  $r^2 = 4$ ,  $\sigma^2 = 1$  and  $n = 100$ .

Adversarial training is optimizing three terms simultaneously (see Eq. (8)). In Section 4, we argued that the  $\ell_2$ -adversarial training when disregarding the middle term is equivalent to ridge regression, and we gave some examples where the estimators are indeed very similar.

Here, however, this third term is needed to explain the behavior we observe. Ridge regression deals with the conflicting goals of optimizing two terms: the parameter  $\ell_2$ -norm and the training error. But, as we in see Fig. 2(a), the training error progressively decays to zero as the number of parameters goes to infinity, only achieving zero error in the limit  $m \rightarrow \infty$ . The adversarial training cost function achieve it after a finite threshold, a behavior that can only be justified by this middle interaction term that appear in Eq. (8) and allow for this abrupt transition.

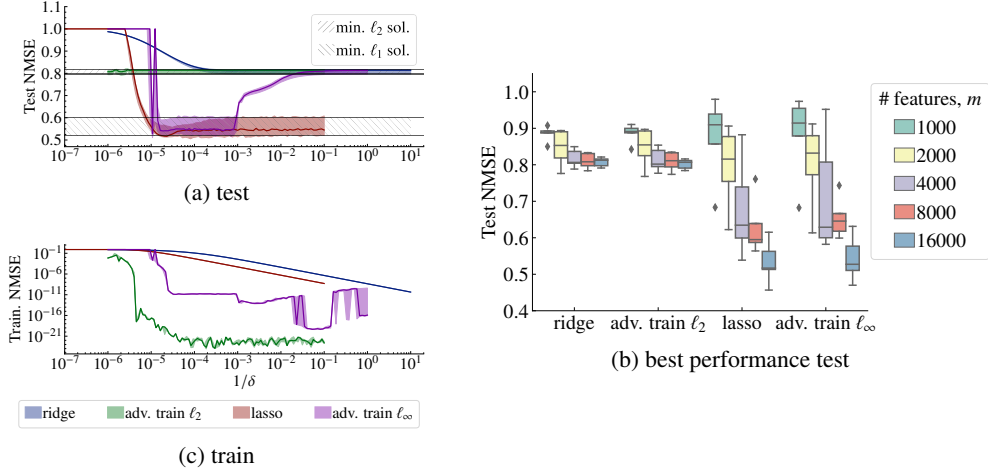


Figure 3: **Results on MAGIC dataset.** The normalized MSE (NMSE) in training and test datasets for each method. The NMSE is defined as the MSE divided by the sample variance of the output variable. In (a) and (c), we fix the number of features  $m = 16000$ . (a) The test NMSE as a function of the regularization parameter is displayed for each method. The median is given by the full line and the interquartile range by the colored region. We also display the performance of minimum  $\ell_1$  and  $\ell_2$ -norm solutions as hashed vertical stripes (interquartile range of the performance). (c) The training NMSE for the same setup. (b) The test NMSE for the best available regularization parameter  $\delta$  obtained via grid search. The number of features  $m$  is indicated in the legend and is indicated by the colors.

The behavior of  $\ell_\infty$ -adversarial training is distinct to that of lasso. Again, while the training error decays progressively with the number of parameters in lasso. For  $\ell_\infty$ -adversarial training there is an abrupt transition where the parameters go to very close to zero. Here the values are sometimes of the order of  $10^{-12}$  and sometimes lower. Monitoring the optimization problem, however, reveals that it seems like the problem that needs to be solved in the  $\ell_\infty$  case is not so well conditioned, which could explain the difference.

## 6.2 Example: phenotype prediction from genotype

We illustrate our method on the genome sequence data from National Institute for Applied Botany (NIAB). The NIAB Diverse MAGIC wheat dataset contain the whole genome sequence data and multiple phenotypes for a population of 504 inbred lines. The NIAB Diverse MAGIC population of winter wheat, which was chosen to maximise the genetic diversity captured from United Kingdom wheat varieties [34]. Here we use the a subset of the genotype to predict one of the continuous phenotypes. We compare adversarial training with lasso and ridge regression. We use half of the individuals ( $n = 252$ ) for training and the remaining 252 samples for testing.

The genetic sequence data contain more 1.1 million SNP (single nucleotide polymorphisms). Each SNP is a binary value indicating whether the given nucleotide differs from the reference value. We use in this example only a pruned version of the genome as input to the model. Closely located SNPs tend to be correlated and hence using a pruned version of the genome can still yield useful predictions. We consider  $m$  features  $m \in \{1000, 2000, 4000, 8000, 16000\}$ , where  $m$  is a subset of the SNPs. The subset is uniform sampled from the genetic sequence data and for each value of  $m$  we repeat the same experiment 5 times with differently sampled features.

Fig. 3 shows the mean square error obtained in predicting the phenotype. Figure (a) and (b) show, respectively, the test and training error as a function of the regularization parameter  $\delta$ . Figure (c) gives the test error (for the best regularization parameter) of each of the methods. In all cases, the confidence intervals are obtained by repeating the experiments for different subset of features sampled from the genetic data.

Fig. 3(c) illustrates again the similarity in performance between ridge regression and  $\ell_2$ -adversarial training, lasso and  $\ell_\infty$ -adversarial training display similar performance. Interestingly, for  $m = 1000$

ridge (and  $\ell_2$ -adversarial training) have the best performance, but as  $m$  increases lasso and  $\ell_\infty$ -adversarial training outperform the rest. That is, they do a better job at incorporating more features without worsening the performance in the test. Interestingly, while the training error decay slowly as we vary the amount of regularization  $\delta$  for lasso and ridge regression. For adversarial training, we see again an abrupt drop in the training error. And after this abrupt drop the model starts to perfectly fit the training dataset (up to numerical precision in the case of  $\ell_2$ ). More interestingly, even when interpolating the training dataset models trained adversarially still perform well on the test set.

### 6.3 Minimum $\ell_2$ and $\ell_1$ -norm solutions.

The minimum  $\ell_2$ -norm solution (that we denote here by  $\hat{\beta}^{\ell_2}$ ), has been often used in studying the role overparametrization in connection with the double-descent phenomena, for instance in [24], [33]. It is the parameter vector that minimizes  $\|\beta\|_2$  subject to  $X\beta = y$ . Another natural alternative is to minimize  $\|\beta\|_1$  subject to same constraint. This second problem is well studied and known as basis pursuit [35] and also has been studied in connection with “benign-overfitting” phenomena in [36]. We denote this solution as  $\hat{\beta}^{\ell_1}$ .

In Fig. 3(a) in the previous page the hatched region provides the interquartile range of test performance obtained by models with the parameters  $\hat{\beta}^{\ell_2}$  and  $\hat{\beta}^{\ell_1}$  obtained over the multiple experiments. We note that the MAGIC dataset is a natural example where the  $\hat{\beta}^{\ell_1}$  can outperform the  $\hat{\beta}^{\ell_2}$  and a counterpoint to the negative properties of it pointed in Chatterji *et al.* [37]. It is well known that the parameter estimated by ridge regression converges to  $\hat{\beta}^{\ell_2}$  as  $\delta \rightarrow 0$ . Fig. 3(a) illustrates that the performance of the two indeed become very similar in the limit. The same can be said for  $\ell_2$ -adversarial training performance. For the  $\ell_\infty$ -adversarial training however, the behavior is less intuitive. It first displays a performance that is close to the performance displayed by the  $\hat{\beta}^{\ell_1}$  then transition *back* into a performance similar to that of the  $\hat{\beta}^{\ell_2}$ .

To further study the phenomena, we take the data generation model described in Section 6.1 with  $m = 200$  and  $n = 60$  fixed and show what happens as we vary  $\delta$ . Fig. 4 shows both the training mean square error and the distance of the estimated parameter to  $\hat{\beta}^{\ell_2}$  and  $\hat{\beta}^{\ell_1}$ . Again we observe, abrupt transition into the interpolation regime for both adversarial training methods. For  $\ell_2$ -adversarial training, the figure shows that as the system abruptly transition into the interpolation regime it get very close to the  $\hat{\beta}^{\ell_2}$ . However, as we further reduce  $\delta$ , the distance from it increases again. For  $\ell_\infty$ -adversarial training, the figure shows that as the system abruptly transitions into the interpolation regime, it get closer to  $\hat{\beta}^{\ell_1}$ . However as we keep decreasing  $\delta$  we see a second transition, now towards the  $\hat{\beta}^{\ell_2}$ . This interesting behavior for the  $\ell_\infty$ -adversarial training was observed for different datasets (see the previous example and also the supplementary material).

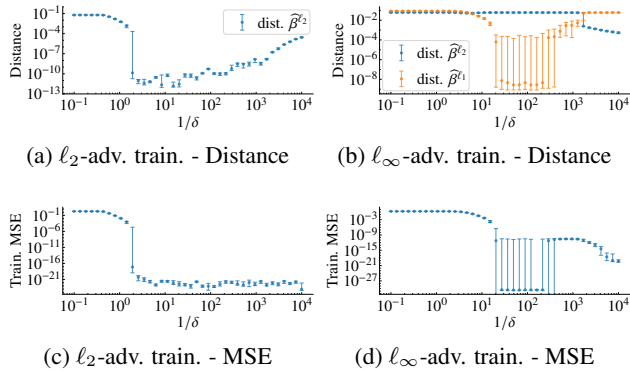


Figure 4: **Distance to minimum norm solutions.** In (a) and (b) we show the distance of the estimated parameter  $\hat{\beta}$  to minimum  $\ell_2$  and  $\ell_1$ -norm solutions, i.e.  $\|\hat{\beta} - \hat{\beta}^{\ell_2}\|_2$  and  $\|\hat{\beta} - \hat{\beta}^{\ell_1}\|_2$ . In (c) and (d) we show the mean square error in the training dataset. The error bars give the median and the 0.25 and 0.75 quantiles obtained from numerical experiment (30 realizations).

### 6.4 Abrupt transitions in behavior

The previous experiments illustrate that adversarial training can go through abrupt transitions in behavior. We show two different ways that we can observe the transition: we fixed the dataset  $n$  and  $\delta$  and kept increasing  $m$  the number of feature in the first example. In the second, we kept decreasing

$\delta$  for a fixed  $m$  and  $n$ . In both cases, the resulting predictors begin to interpolate the training data abruptly beyond a certain threshold.

Equation (7) gives it own insight into why abrupt transitions occur. We focus on the  $\ell_2$ -adversarial case and define  $f_i(\beta) = |y_i - x_i^\top \beta| + \delta \|\beta\|_2$ . Eq. (7) can then be stated as  $\widehat{R}_2^{\text{adv}}(\beta) = \frac{1}{n} \sum_{i=1}^n f_i(\beta)^2$ . Analysing the function  $f_i$  can be instructive.

Notice that given an arbitrary  $\beta$  can be decomposed in two parts, one perpendicular to  $x_i$  and another one parallel to it. For instance, if we let  $v_i = \text{sign}(y_i) \frac{x_i}{\|x_i\|}$  then we can write  $\beta = \alpha v_i + \beta_\perp$ , where we denoted the perpendicular component as  $\beta_\perp$ . Since the two components are perpendicular we have that  $\|\beta\|_2 > \alpha$  as long as  $\beta_\perp \neq 0$  and that  $f_i(\alpha v_i) \leq f_i(\beta)$ . Hence the function is necessarily minimized along the subspace spanned by the vector  $v_i$ . Now along this line, the function  $f_i$  is piecewise linear with three segments. We show the function in Fig. 5 for different values of  $\delta$ . It is easy to understand why of the abrupt transition by looking at this function: one of the three segments change slope sign as we change  $\delta$  and the minimum of the function changes abruptly.

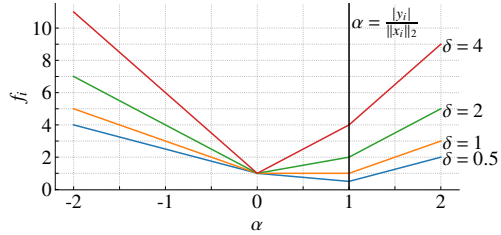


Figure 5: **Function  $f_i$ .** The plot was generated for  $|y_i| = \|x_i\|_2 = 1$  and for different values of  $\delta$ . For  $\delta > \|x_i\|_2$  the function has a minima at  $\alpha = |y_i|/\|x_i\|_2$ . For,  $\delta < \|x_i\|_2$  it has a minima at  $\alpha = 0$ . For  $\delta = \|x_i\|_2$  the function has a segment with slope 0 and is minimized at all the points in this segment

## 7 Conclusion and future work

This work opens many possibilities. We believe *adversarial training for linear models* can have many applications and is interesting on its own right, not only as an intermediary step in getting insight into more complex models. The case where there are more features than parameters occurs quite frequently in computational biology. Lasso, elastic net [38] and many other estimators are commonly used in such problems, but having an estimator with new properties could enable new applications and analysis. As we show here, adversarial training has the interesting property of regularizing the solution while capable interpolating the training data. Moreover, the regularization parameter  $\delta$  has the clear interpretation of allowing a robust region around the regressors.

We also note that adversarial training is a potentially interesting method for dealing with errors-in-variables, i.e., cases where there are measurement errors for the input  $x$ . By considering an adversary that generates the worst possible case of errors-in-variables, it would be natural to expect that less pathological cases could also be improved. We note that for a sufficiently large  $\delta$ , even if  $x$  is noisy version of the true input value  $x^*$ , we would still have  $x^*$  inside the region the adversary is constrained to. Errors-in-variable problems are of interest to applications that range from economic analysis [39] to process control [40]. These problems also appear naturally in causal inference. For instance, in conditional average treatment effect, the attempt to eliminate confounding effects naturally introduce errors in the measurements. Other connections are also possible, the adversarial risk defined in Eq. (2) is an interesting case where there is a distribution shift on the input and the shift itself depends on the parameter. Cases where the distribution shift depends on the parameter are of interest in policy-making. See a formulation in Perdomo *et al.* [41].

We point that more technical developments are still needed to make the method practical. While convex, the optimization is still quite inefficient. Coordinate descent [32], [42] and LARS [29] are clever solutions that allow the entire regularization path to be efficiently estimated for lasso and elastic net. Having tailored solvers for linear adversarial training could also make this method more computationally attractive and useful. Finally, the empirical finds of Section 6 are interesting but still need further study. We observe a sharp transition into interpolation and show there is some connections with the  $\ell_1$  and  $\ell_2$  minimum norm solutions. We intend to study and formalize these ideas in future work.

## Acknowledgments and Disclosure of Funding

The authors would like to thank Carl Nettelblad for very fruitful discussions throughout the work with this research. This research was financially supported by the *Kjell och Märta Beijer Foundation* and by the Swedish Research Council through the projects: *Deep probabilistic regression – new models and learning algorithms* (contract number: 2021-04301) and *Counterfactual Prediction Methods for Heterogeneous Populations* (contract number: 2018-05040).

## References

- [1] J. Bruna, C. Szegedy, I. Sutskever, I. Goodfellow, W. Zaremba, R. Fergus, and D. Erhan, “Intriguing properties of neural networks,” in *Proceedings of the 2nd International Conference on Learning Representations (ICLR)*, 2014.
- [2] I. J. Goodfellow, J. Shlens, and C. Szegedy, “Explaining and Harnessing Adversarial Examples,” in *Proceedings of the 3rd International Conference on Learning Representations (ICLR)*, 2015.
- [3] A. Kurakin, I. Goodfellow, S. Bengio, *et al.*, “Adversarial Attacks and Defences Competition,” *arXiv:1804.00097*, 2018.
- [4] A. Fawzi, O. Fawzi, and P. Frossard, “Analysis of classifiers’ robustness to adversarial perturbations,” *Machine Learning*, vol. 107, no. 3, pp. 481–508, 2018.
- [5] A. Ilyas, S. Santurkar, D. Tsipras, L. Engstrom, B. Tran, and A. Madry, “Adversarial Examples Are Not Bugs, They Are Features,” *Advances in Neural Information Processing Systems*, vol. 32, 2019.
- [6] X. Yuan, P. He, Q. Zhu, and X. Li, “Adversarial examples: Attacks and defenses for deep learning,” *IEEE transactions on neural networks and learning systems*, vol. 30, no. 9, pp. 2805–2824, 2019.
- [7] N. Dalvi, P. Domingos, Mausam, S. Sanghai, and D. Verma, “Adversarial classification,” in *Proceedings of the tenth ACM SIGKDD international conference on knowledge discovery and data mining*, 2004.
- [8] A. Globerson and S. Roweis, “Nightmare at test time: Robust learning by feature deletion,” in *Proceedings of the 23rd international conference on Machine learning (ICML)*, 2006, pp. 353–360.
- [9] A. Madry, A. Makelov, L. Schmidt, D. Tsipras, and A. Vladu, “Towards Deep Learning Models Resistant to Adversarial Attacks,” *Proceedings of the International Conference for Learning Representations (ICLR)*, 2018.
- [10] R. Huang, B. Xu, D. Schuurmans, and C. Szepesvari, “Learning with a Strong Adversary,” *arXiv:1511.03034*, 2016.
- [11] T. Bai, J. Luo, J. Zhao, B. Wen, and Q. Wang, “Recent Advances in Adversarial Training for Adversarial Robustness,” *arXiv:2102.01356*, 2021.
- [12] A. H. Ribeiro and T. B. Schön, “Overparameterized Linear Regression under Adversarial Attacks,” *arXiv:2204.06274*, 2022.
- [13] H. Taheri, R. Pedarsani, and C. Thrampoulidis, “Asymptotic Behavior of Adversarial Training in Binary Classification,” *arXiv:2010.13275*, 2021.
- [14] A. Javanmard, M. Soltanolkotabi, and H. Hassani, “Precise tradeoffs in adversarial training for linear regression,” in *Proceedings of 33rd Conference on Learning Theory*, vol. 125, PMLR, 2020, pp. 2034–2078.
- [15] A. Javanmard and M. Soltanolkotabi, “Precise Statistical Analysis of Classification Accuracies for Adversarial Training,” *arXiv:2010.11213*, 2020.
- [16] H. Hassani and A. Javanmard, “The curse of overparametrization in adversarial training: Precise analysis of robust generalization for random features regression,” *arXiv:2201.05149*, 2022.
- [17] Y. Min, L. Chen, and A. Karbasi, “The Curious Case of Adversarially Robust Models: More Data Can Help, Double Descend, or Hurt Generalization,” *Proceedings of the Thirty-Seventh Conference on Uncertainty in Artificial Intelligence*, vol. 161, pp. 129–139, 2021.
- [18] D. Yin, R. Kannan, and P. Bartlett, “Rademacher Complexity for Adversarially Robust Generalization,” in *Proceedings of the 36th International Conference on Machine Learning*, PMLR, 2019, pp. 7085–7094.

- [19] Y. Guo, C. Zhang, C. Zhang, and Y. Chen, “Sparse DNNs with Improved Adversarial Robustness,” in *Advances in Neural Information Processing Systems*, vol. 31, 2018.
- [20] S. Gopalakrishnan, Z. Marzi, U. Madhow, and R. Pedarsani, “Combating Adversarial Attacks Using Sparse Representations,” *arXiv:1803.03880*, 2018.
- [21] Y. Xing, R. Zhang, and G. Cheng, “Adversarially robust estimate and risk analysis in linear regression,” in *Proceedings of the 24th international conference on artificial intelligence and statistics*, ser. Proceedings of machine learning research, vol. 130, PMLR, 2021, pp. 514–522.
- [22] H. Xu, C. Caramanis, and S. Mannor, “Robust regression and lasso,” *Advances in neural information processing systems*, vol. 21, 2008.
- [23] U. Shaham, Y. Yamada, and S. Negahban, “Understanding adversarial training: Increasing local stability of supervised models through robust optimization,” *Neurocomputing*, vol. 307, pp. 195–204, 2018.
- [24] M. Belkin, D. Hsu, S. Ma, and S. Mandal, “Reconciling modern machine-learning practice and the classical bias–variance trade-off,” *Proceedings of the National Academy of Sciences*, vol. 116, no. 32, pp. 15 849–15 854, 2019.
- [25] C. Zhang, S. Bengio, M. Hardt, B. Recht, and O. Vinyals, “Understanding deep learning requires rethinking generalization,” in *Proceedings of the 5th International Conference on Learning Representations (ICLR)*, 2017.
- [26] P. L. Bartlett, P. M. Long, G. Lugosi, and A. Tsigler, “Benign overfitting in linear regression,” *Proceedings of the National Academy of Sciences*, vol. 117, no. 48, pp. 30 063–30 070, 2020.
- [27] P. L. Bartlett, A. Montanari, and A. Rakhlin, “Deep learning: A statistical viewpoint,” *arXiv:2103.09177*, 2021.
- [28] D. Tsipras, S. Santurkar, L. Engstrom, A. Turner, and A. Ma, “Robustness May Be At Odds with Accuracy,” *Proceedings of the International Conference for Learning Representations (ICLR)*, p. 23, 2019.
- [29] B. Efron, T. Hastie, I. Johnstone, and R. Tibshirani, “Least angle regression,” *The Annals of Statistics*, vol. 32, no. 2, pp. 407–499, 2004.
- [30] R. Tibshirani, “Regression shrinkage and selection via the LASSO,” *Journal of the Royal Statistical Society. Series B (Methodological)*, pp. 267–288, 1996.
- [31] S. Diamond and S. Boyd, “CVXPY: A Python-embedded modeling language for convex optimization,” *Journal of Machine Learning Research*, vol. 17, no. 83, pp. 1–5, 2016.
- [32] J. Friedman, T. Hastie, and R. Tibshirani, “Regularization paths for generalized linear models via coordinate descent,” *Journal of statistical software*, vol. 33, no. 1, p. 1, 2010.
- [33] T. Hastie, A. Montanari, S. Rosset, and R. J. Tibshirani, “Surprises in High-Dimensional Ridgeless Least Squares Interpolation,” *arXiv:1903.08560*, 2019.
- [34] M. F. Scott, N. Fradgley, A. R. Bentley, *et al.*, “Limited haplotype diversity underlies polygenic trait architecture across 70 years of wheat breeding,” *Genome Biology*, vol. 22, no. 1, p. 137, 2021.
- [35] S. S. Chen, D. L. Donoho, and M. A. Saunders, “Atomic decomposition by basis pursuit,” *SIAM Journal on Scientific Computing*, vol. 20, no. 1, pp. 33–61, 1998.
- [36] G. Wang, K. Donhauser, and F. Yang, “Tight bounds for minimum  $l_1$ -norm interpolation of noisy data,” *arXiv:2111.05987*, 2022.
- [37] N. S. Chatterji and P. M. Long, “Foolish Crowds Support Benign Overfitting,” *arXiv:2110.02914*, 2022.
- [38] H. Zou and T. Hastie, “Regularization and Variable Selection via the Elastic Net,” *Journal of the Royal Statistical Society. Series B (Statistical Methodology)*, vol. 67, no. 2, pp. 301–320, 2005.
- [39] C.-L. Cheng and J. W. Van Ness, “Errors in variables in econometrics,” in *Econometrics in theory and practice: Festschrift for hans schneeweiss*, Heidelberg: Physica-Verlag HD, 1998, pp. 3–13.
- [40] T. Söderström, “Errors-in-variables methods in system identification,” *Automatica*, vol. 43, no. 6, pp. 939–958, 2007.
- [41] J. Perdomo, T. Zrnic, C. Mendler-Dünner, and M. Hardt, “Performative prediction,” in *Proceedings of the 37th international conference on machine learning*, ser. Proceedings of machine learning research, vol. 119, PMLR, 2020, pp. 7599–7609.

- [42] J. Friedman, T. Hastie, H. Höfling, and R. Tibshirani, “Pathwise coordinate optimization,” *The Annals of Applied Statistics*, vol. 1, no. 2, pp. 302–332, 2007.
- [43] S. P. Boyd and L. Vandenberghe, *Convex optimization*. Cambridge University Press, 2004.

## Supplementary Material

# Surprises in adversarially-trained linear regression

## A Proofs

### A.1 Proof of Lemma 2

Following Ribeiro *et al.* [12] we provide a proof of Lemma 2, but before we do that we will restate a well-known proposition that will be useful. Most adversarial attacks are in fact constructed based on this proposition.

**Proposition 6.** *Given  $p, q \in (1, \infty)$  such that  $1/p + 1/q = 1$  and  $\beta \in \mathbb{R}^m$ ,  $\Delta x \in \mathbb{R}^m$ . We have  $|\beta^\top \Delta x| = \|\beta\|_p \|\Delta x\|_q$  when the  $i^{\text{th}}$  component is  $\Delta x_i = |\beta_i|^{q/p}$ . Moreover, if  $\Delta x_i = \text{sign}(\beta_i)$  for every  $i$ , then  $|\beta^\top \Delta x| = \|\beta\|_\infty \|\Delta x\|_1$ , and if*

$$\Delta x_i = \frac{s_i}{\sum_i s_i} \quad \text{for} \quad s_i = \begin{cases} 1 & \text{if } \beta_i = \max_i \beta_i \\ 0 & \text{otherwise} \end{cases}$$

then  $|\beta^\top \Delta x| = \|\beta\|_1 \|\Delta x\|_\infty$ .

With this proposition at hand we are ready to prove the Lemma. For  $1 \leq p \leq \infty$ , let  $q$  be a positive real number for which  $\frac{1}{p} + \frac{1}{q} = 1$ . Let  $e_0 = y_0 - x_0^\top \beta$ . The adversarial risk (2) can—after some algebraic manipulation—be rewritten as

$$R_p^{\text{adv}}(\beta) = \mathbb{E}_{x_0, y_0} \left[ e_0^2 + \max_{\|\Delta x_0\|_p \leq \delta} ((\Delta x_0^\top \beta)^2 - 2e_0 \Delta x_0^\top \beta) \right]$$

In turn, if we let  $r = \Delta x_0^\top \beta$  since  $\|\Delta x_0\|_p \leq \delta$ , Hölder’s inequality yields  $|r| \leq \delta \|\beta\|_q$ , for  $q$  satisfying  $1/p + 1/q = 1$ . Since Proposition 6 guarantees we that can always choose vectors such that the equality holds, the term inside the expectation of the right hand side is equal to:  $M = \max_{|r| \leq \delta \|\beta\|_q} (r^2 - 2e_0 r)$ . Now the maximum is obtained for  $r = -\delta \|\beta\|_q$  if  $e_0 \geq 0$  and at  $r = \delta \|\beta\|_q$  if  $e_0 < 0$ , hence  $M = \delta^2 \|\beta\|_q^2 + 2\delta \|\beta\|_q |e_0|$ . We now have that

$$R_p^{\text{adv}}(\beta) = \mathbb{E}_{x_0, y_0} \left[ \delta^2 \|\beta\|_q^2 + 2\delta \|\beta\|_q |e_0| + |e_0|^2 \right], \quad (\text{S.1})$$

and the result follows.

### A.2 Proof Proposition 3

Let  $\gamma \in [0, 1]$ , for  $q \in [1, \infty]$ ,  $\|\beta\|_q$  is a norm and from the triangular inequality we have that:

$$\|\gamma \beta_1 + (1 - \gamma) \beta_2\|_q \leq \gamma \|\beta_1\|_q + (1 - \gamma) \|\beta_2\|_q. \quad (\text{S.2})$$

Moreover,

$$|y_0 - x_0^\top (\gamma \beta_1 + (1 - \gamma) \beta_2)| \leq \gamma |y_0 - x_0^\top \beta_1| + (1 - \gamma) |y_0 - x_0^\top \beta_2|.$$

Hence,  $h(\beta) = |y_0 - x_0^\top \beta| + \|\beta\|_q$  is convex and,  $h(\beta) \geq 0$  for all  $\beta$ . Now, since  $g(x) = x^2$  is convex and non-decreasing for  $x \geq 0$ , the composition  $g \circ h$  is convex – See Boyd *et al.* [43, Section 3.2.4]; moreover, the expected value of a convex function is also convex [43, Section 3.2.1] and it follows that the right-hand side of Eq. (6) is convex.

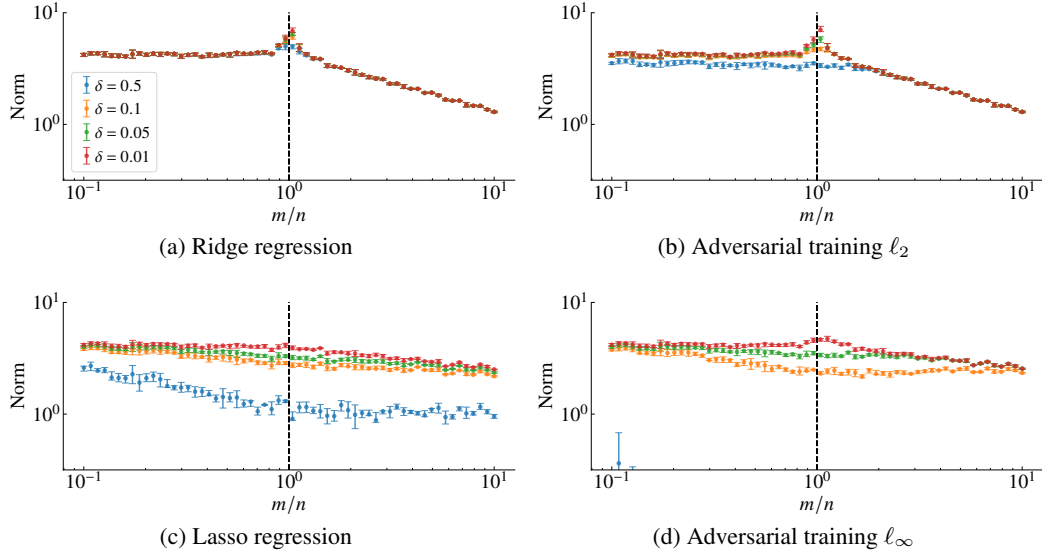


Figure S.1: **Parameter  $\ell_2$ -norm: isotropic case.** We plot  $\|\hat{\beta}\|_2$  for the parameters estimated by the different methods. The setup is exactly the same as Fig. 2. In (d), the norm for  $\delta = 0.5$  becomes very close to zero  $\approx 10^{-10}$ , we let it leave the region in the plot so it is possible to better visualize the curves for the other regularization parameters.

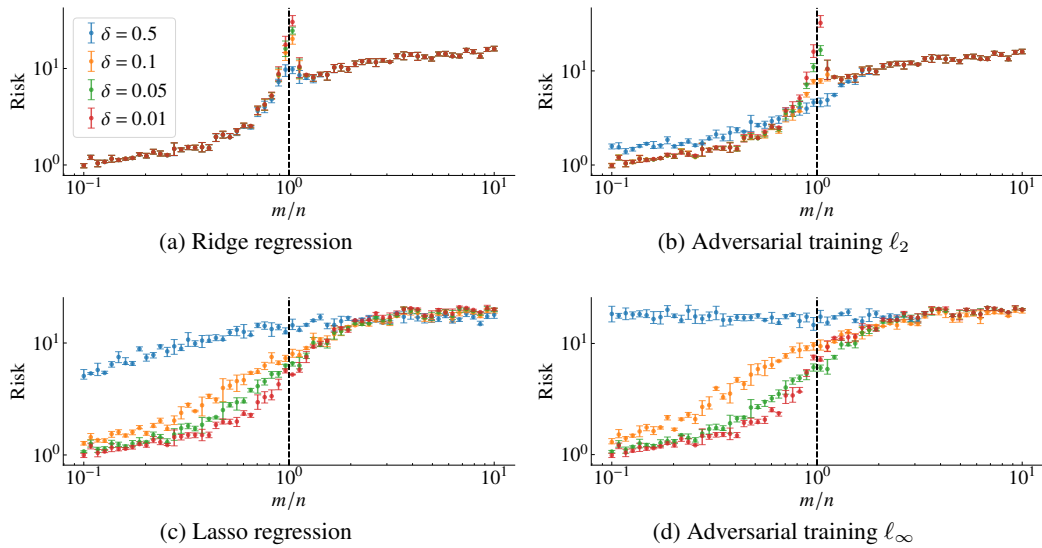


Figure S.2: **Test MSE: isotropic case.** We plot the MSE in a test dataset of size  $n_{\text{test}} = 100$  for the parameters estimated by the different methods. The setup is exactly the same as in Fig. 2.

## B Isotropic feature models: Additional plots

Here we include additional plots related to Section 6.1. Fig. S.1 show the parameter  $\ell_2$ -norm and Fig. S.2 show the performance on a hold-out test set.

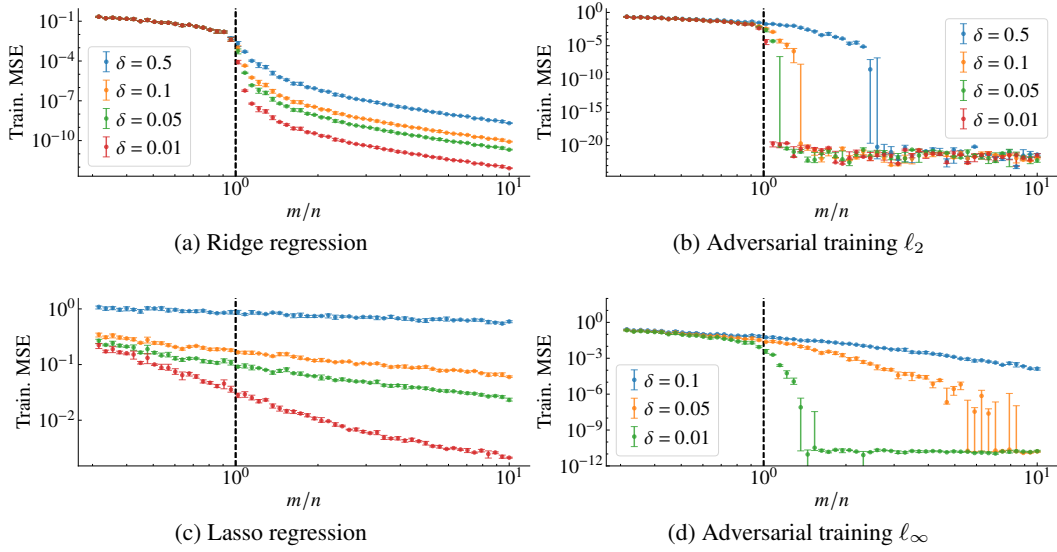


Figure S.3: **Mean square error in training data: latent features.** The plot is equivalent to Fig. 2 but with a different data generation procedure. The error bars give the median and the 0.25 and 0.75 quantiles obtained from numerical experiments (6 realizations) and for regularization parameter  $\delta = \{0.5, 0.1, 0.05, 0.01\}$  with the colors corresponding to each case indicated in the legend. In (d), we omit the plot for  $\delta = 0.5$ , that is because for this high regularization the solver becomes ill-conditioned.

## C Latent feature models

Let us assume that the features are generated using the latent space feature model described in Hastie *et al.* [33, Section 5.4]. Here, the features  $x$  are noisy observations of a lower-dimensional subspace of dimension  $d$ . A vector in this *latent space* is represented by  $z \in \mathbb{R}^d$ . This vector is indirectly observed via the features  $x \in \mathbb{R}^m$  according to

$$x = Wz + u, \quad (\text{S.3})$$

where  $W$  is an  $m \times d$  matrix, for  $m \leq d$ . We assume that the responses are described by a linear model in this latent space

$$y = \theta^\top z + \xi, \quad (\text{S.4})$$

where  $\xi \in \mathbb{R}$  and  $u \in \mathbb{R}^m$  are mutually independent noise variables. Moreover,  $\xi \sim \mathcal{N}(0, \sigma_\xi^2)$  and  $u \sim \mathcal{N}(0, I_m)$ . As in Hastie *et al.* [33], we consider the features in the latent space to be isotropic and normal  $z_i = \mathcal{N}(0, I_d)$  and choose  $W$  such that its columns are orthogonal,  $W^\top W = \frac{m}{d} I_d$ , where the factor  $\frac{m}{d}$  is introduced to guarantee that the signal-to-noise ratio of the feature vector  $x$  (i.e.  $\frac{\|Wz_i\|_2^2}{\|u_i\|_2^2}$ ) is kept constant.

Here we show experiments for  $\sigma_\xi = 0.1$  and  $d = 20$ . All the experiments are analogous to the experiments performed for the isotropic case. Fig. S.3 shows the training mean square error (MSE) of the learned predictors. We keep the number of training datapoints constant and vary the number of features  $m$ . Fig. S.4 show the parameter  $\ell_2$ -norm and Fig. S.5 show the performance on a separate test set. Fig. S.6 use  $m = 200$  and  $n = 60$  fixed and show what happens as we vary  $\delta$ . Fig. S.6 shows both the training mean square error and the distance of the estimated parameter to  $\hat{\beta}^{\ell_2}$  and  $\hat{\beta}^{\ell_1}$ .

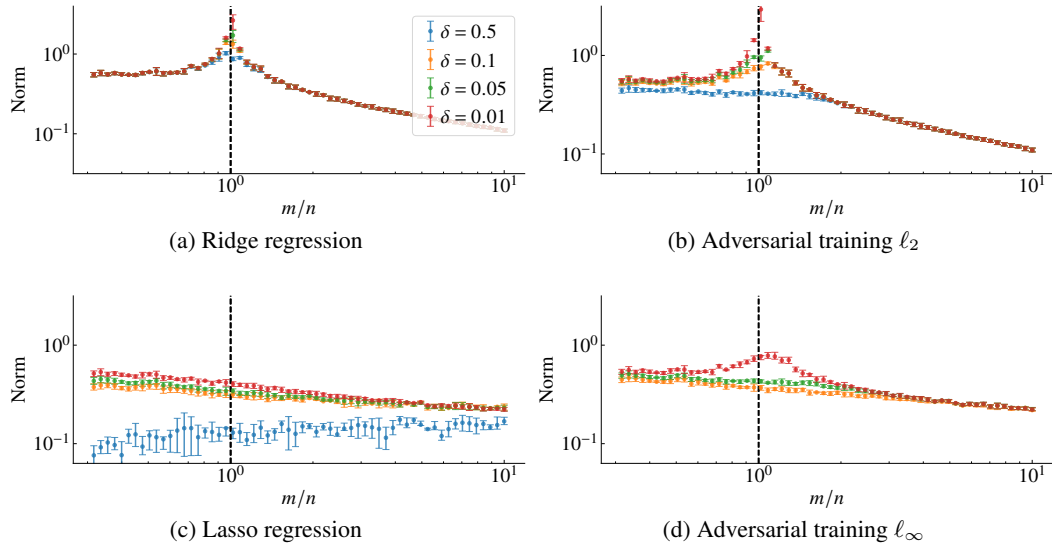


Figure S.4: **Parameter  $\ell_2$ -norm: latent feature model.** We plot  $\|\hat{\beta}\|_2$  for the parameters estimated by the different methods. The setup is exactly the same as Fig. S.3.

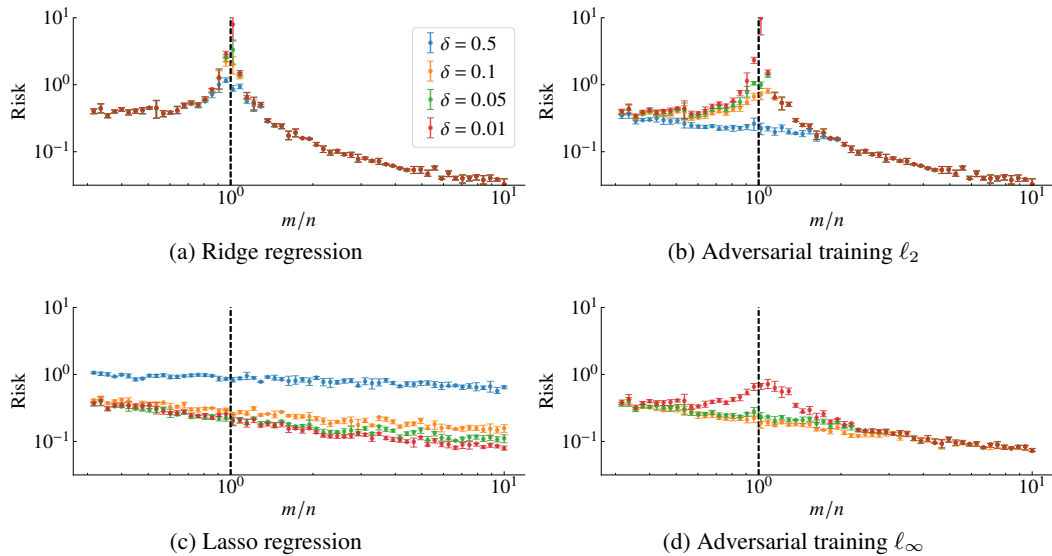


Figure S.5: **Test MSE: latent feature model.** We plot the MSE in a test dataset of size  $n_{\text{test}} = 100$  for the parameters estimated by the different methods. The setup is exactly the same as Fig. S.3.

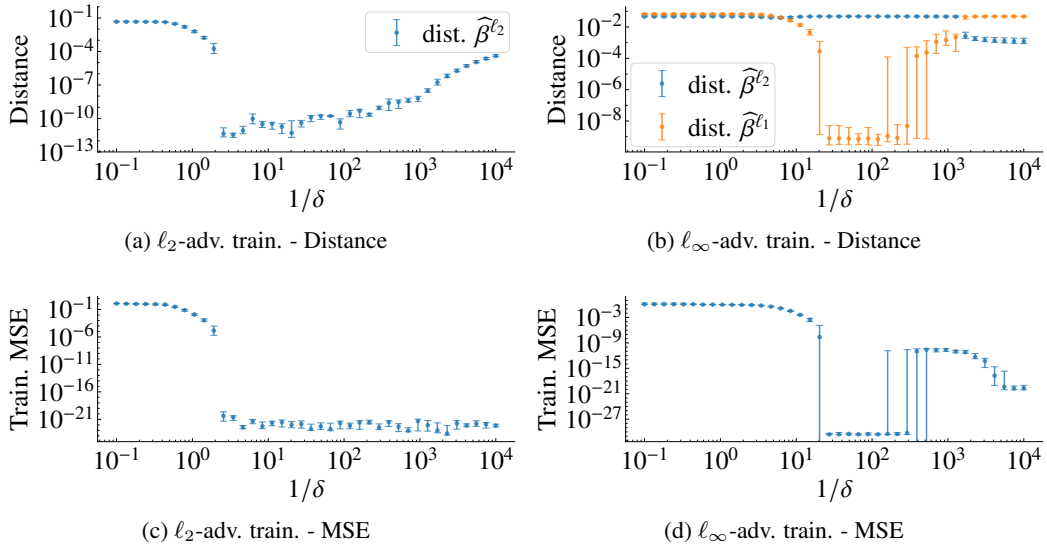


Figure S.6: **Distance to minimum norm solutions: latent feature model.** Equivalent of Fig. 4, but for the latent feature model. In (a) and (b) we show the distance of the estimated parameter  $\widehat{\beta}$  to minimum  $\ell_2$  and  $\ell_1$ -norm solutions, i.e.  $\|\widehat{\beta} - \widehat{\beta}^{\ell_2}\|_2$  and  $\|\widehat{\beta} - \widehat{\beta}^{\ell_1}\|_2$ . In (c) and (d) we show the mean square error in the training dataset. The error bars give the median and the 0.25 and 0.75 quantiles obtained from numerical experiments (30 realizations).